Supporting Information

Porous nanofiber composite membrane with 3D interpenetrating highways towards ultrafast and isotropic proton conduction

Yafang Zhang[a,1], Xiang Zhang[a,1], Ping Li[a], Wenjia Wu[a,b,*], Jianlong Lin[a], Jingtao Wang[a,c,*], Lingbo Qu[b], Haoqin Zhang[a]

[a]School of Chemical Engineering, Zhengzhou University, Zhengzhou 450001, P. R. China

[b]College of Chemistry, Zhengzhou University, Zhengzhou 450001, P. R. China

[c]Henan Institute of Advanced Technology, Zhengzhou University, 97 Wenhua Road Zhengzhou 450003, P.R. China

*To whom correspondence should be addressed: E-mail: wenjiawu@zzu.edu.cn (W.J. Wu); jingtaowang@zzu.edu.cn (J.T. Wang).

[1]These authors contributed equally to this work.

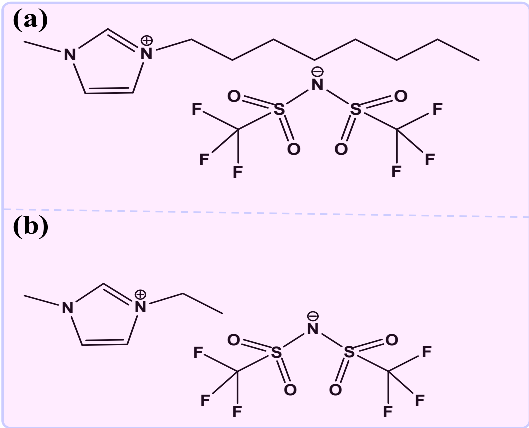

Fig. S1. Chemical structure of ILs: (a) Long alkyl chain [C_8mim][Tf_2N] and (b) short alkyl chain [C_2mim][Tf_2N].

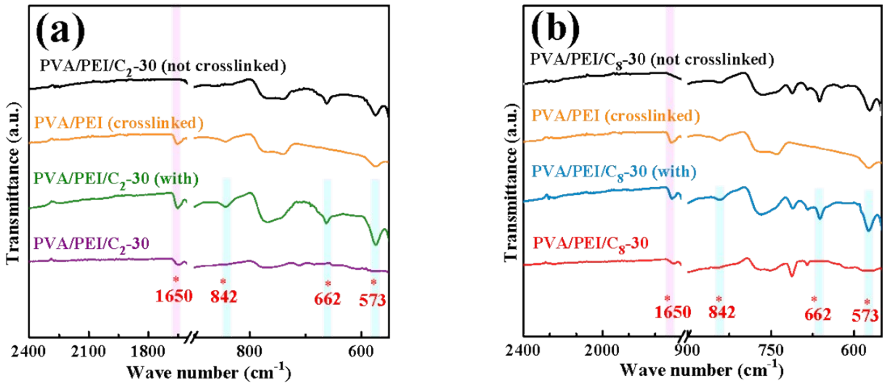

Fig. S2. (a) FTIR spectra of PVA/PEI/C_2-30 (not crosslinked), PVA/PEI (crosslinked), PVA/PEI/C_2-30 (with), and PVA/PEI/C_2-30. (b) FTIR spectra of PVA/PEI/C_8-30 (not crosslinked), PVA/PEI (crosslinked), PVA/PEI/C_8-30 (with), and PVA/PEI/C_8-30.

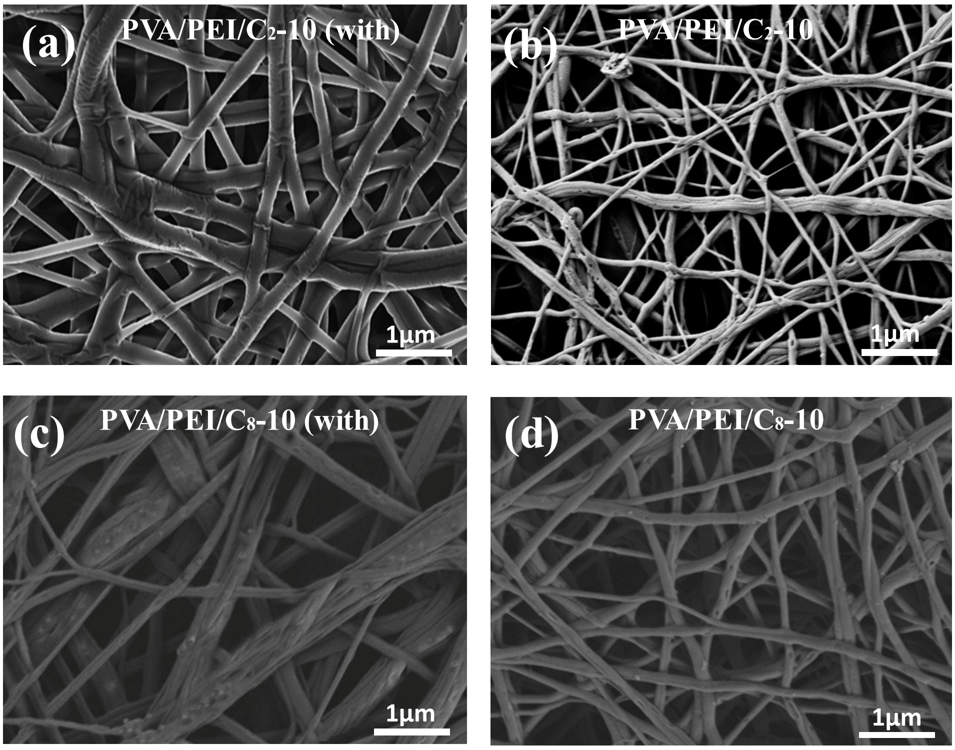

Fig. S3. SEM images of (a) PVA/PEI/C_2-10 (with), (b) PVA/PEI/C_2-10, (c) PVA/PEI/C_8-10 (with), and (d) PVA/PEI/C_8-10.

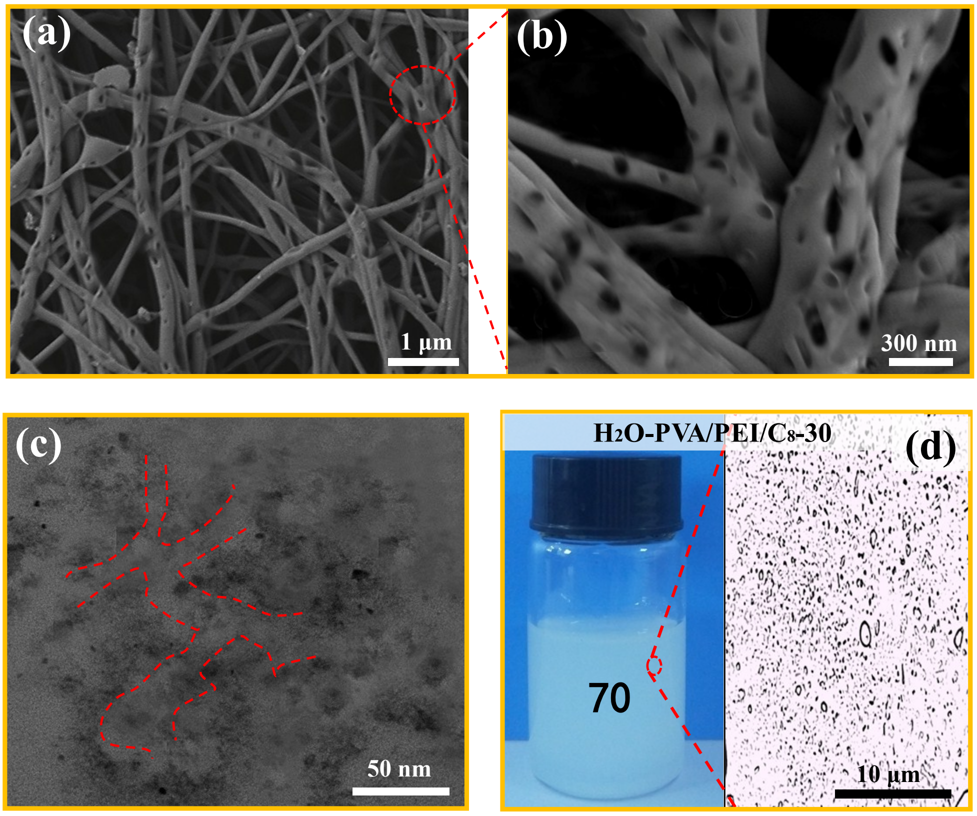

Fig. S4. (a and b) SEM images of PVA/PEI/C_8-30. (c) Cross-sectional TEM image of PVA/PEI/C_8-30. (d) Optical photograph and microscope image of PVA/PEI/C_8-30 electrospinning solution.

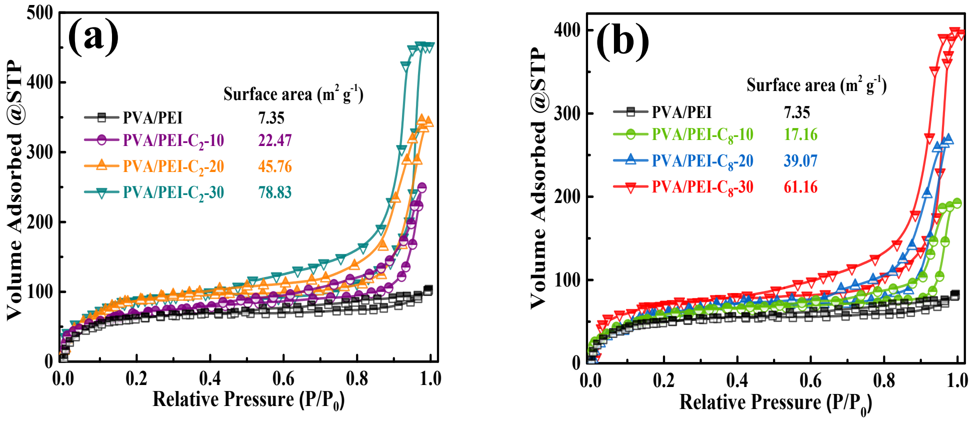

Fig. S5. Nitrogen adsorption/desorption isotherms of (a) PVA/PEI and PVA/PEI/C_2-*Y* and (b) PVA/PEI/C_8-*Y*.

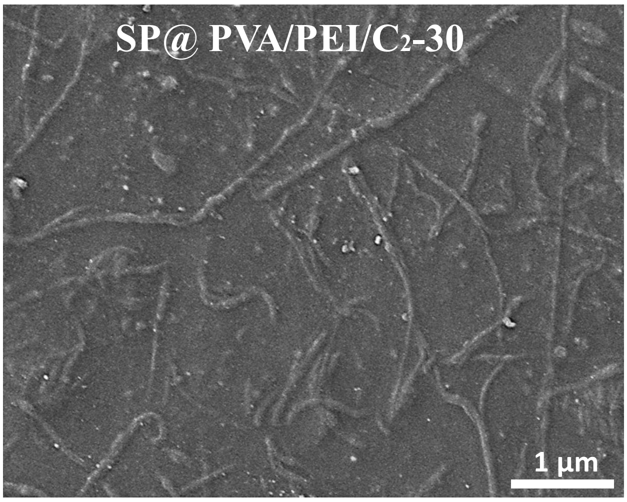

Fig. S6. SEM image of SP@PVA/PEI/C_2-30.

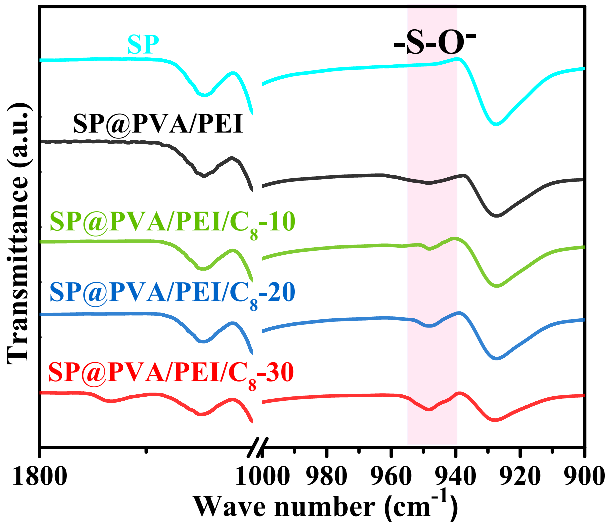

Fig. S7. FTIR spectra of SP, SP@PVA/PEI, and SP@PVA/PEI/C_8-*Y*.

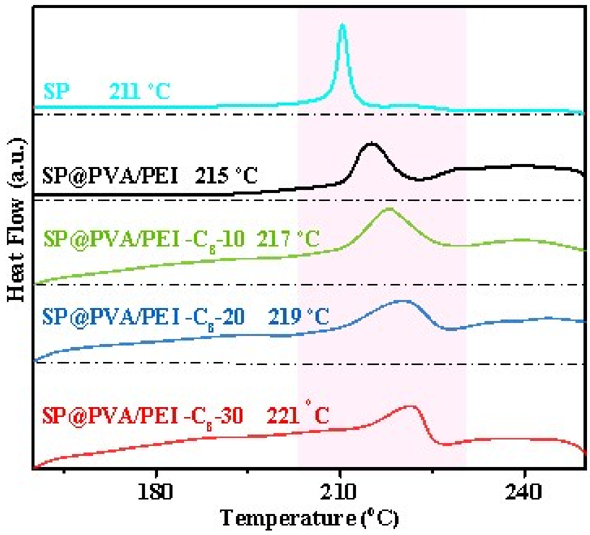

Fig. S8. DSC curves of SP, SP@PVA/PEI, and SP@PVA/PEI/C_8-*Y*.

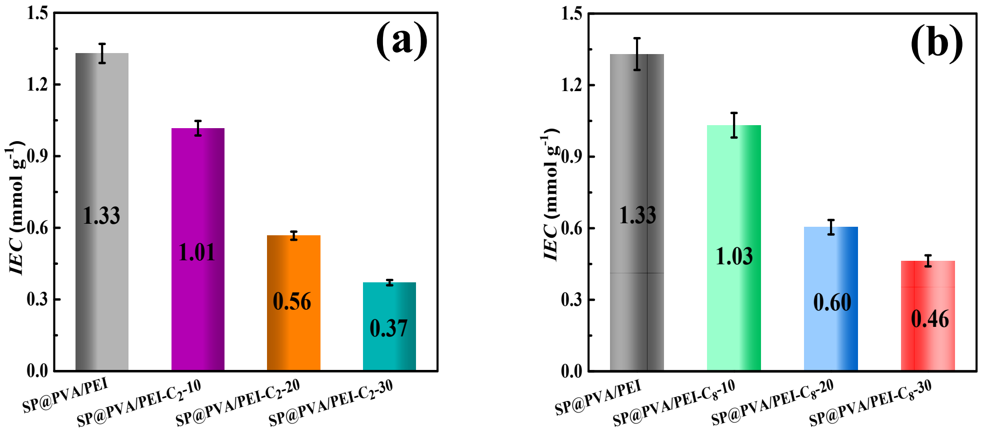

Fig. S9. *IEC* values of (a) SP@PVA/PEI and SP@PVA/PEI/C_2-*Y* and (b) SP@PVA/PEI/C_8-*Y*.

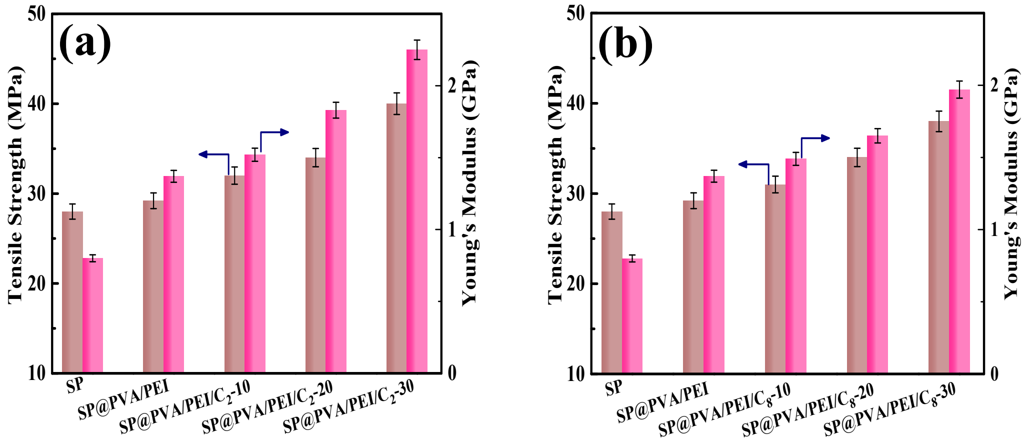

Fig. S10. Mechanical properties of (a) SP, SP@PVA/PEI, SP@PVA/PEI/C_2-Y and (b) SP@PVA/PEI/C_8-Y (note: error bars represent standard deviations for three measurements).

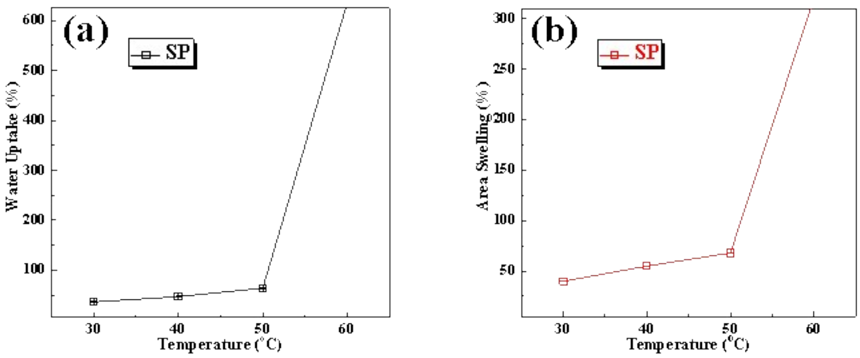

Fig. S11. (a) Water uptake and (b) area swelling of SP.

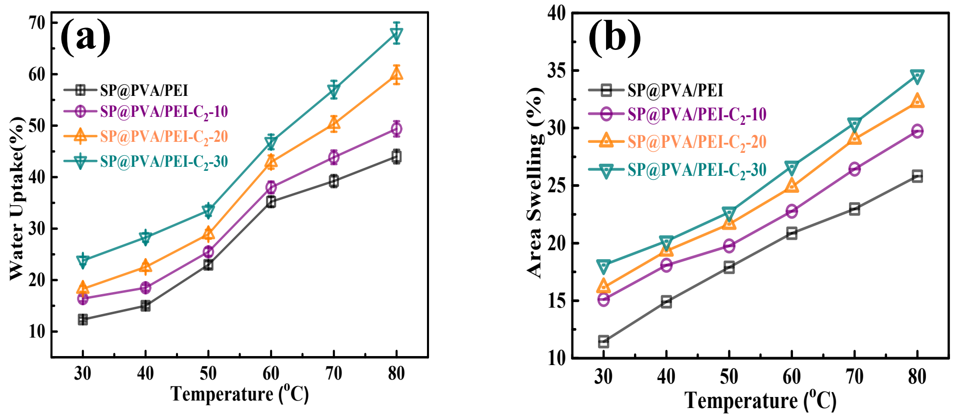

Fig. S12. (a) Water uptake and (b) area swelling of SP@PVA/PEI and SP@PVA/PEI/C_2-*Y*.

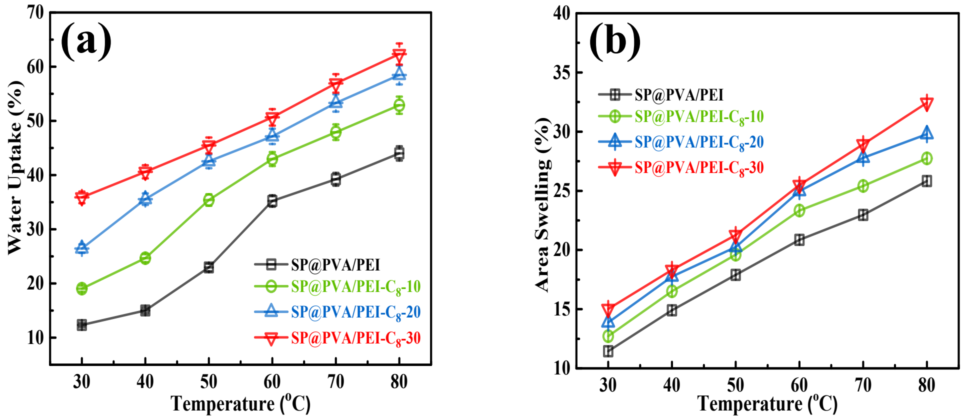

Fig. S13. (a) Water uptake and (b) area swelling of SP@PVA/PEI and SP@PVA/PEI/C_8-*Y*.

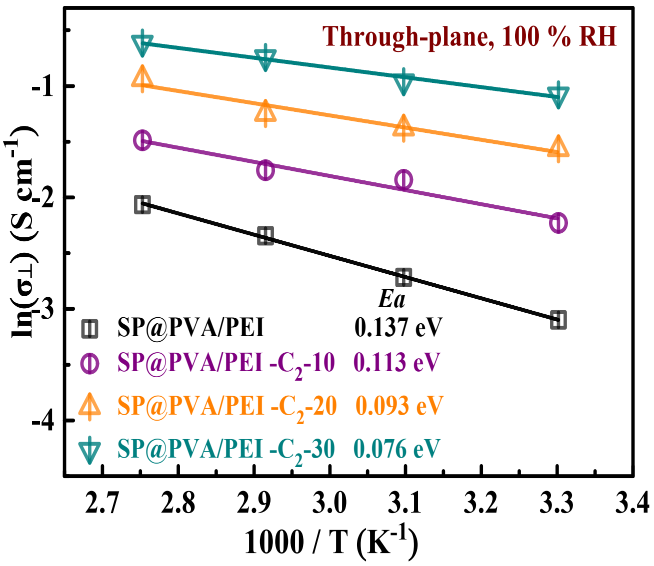

Fig. S14. Arrhenius-plots of through-plane conductivity ($\sigma_{\perp}$) for SP@PVA/PEI and SP@PVA/PEI/C_2-*Y* under 100% RH.

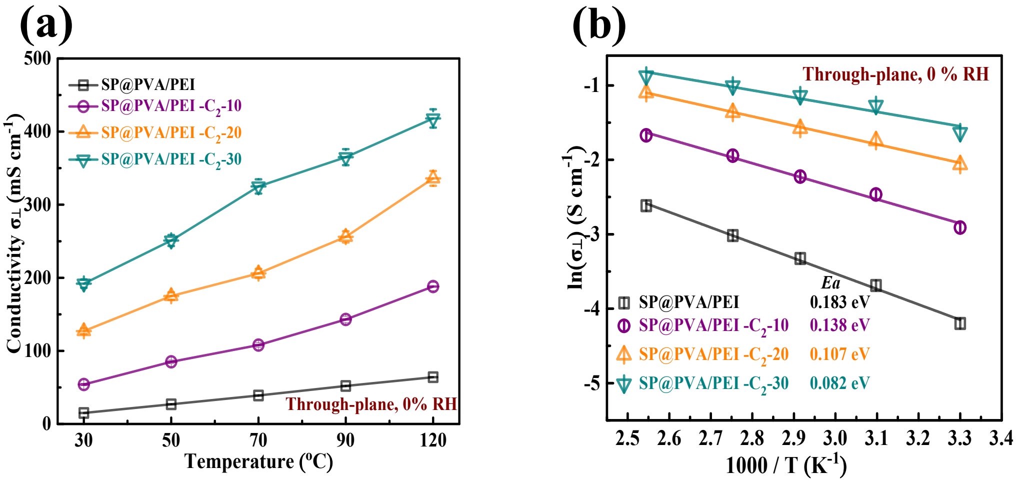

Fig. S15. (a) Temperature-dependent through-plane conductivity ($\sigma_{\perp}$) of SP@PVA/PEI and SP@PVA/PEI/C_2-*Y* under 0% RH. (b) Arrhenius-plots of through-plane conductivity ($\sigma_{\perp}$) under 0% RH.

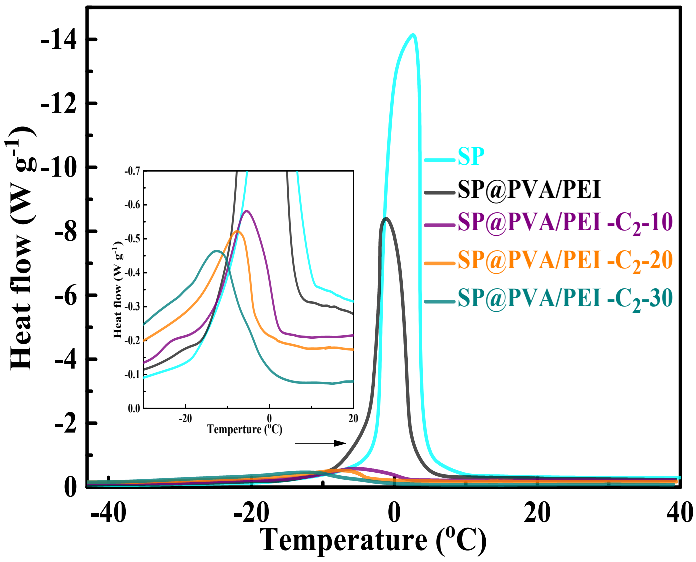

Fig. S16. DSC heating traces of SP, SP@PVA/PEI, and SP@PVA/PEI/C_2-*Y* (note: inset is the magnification of DSC traces).

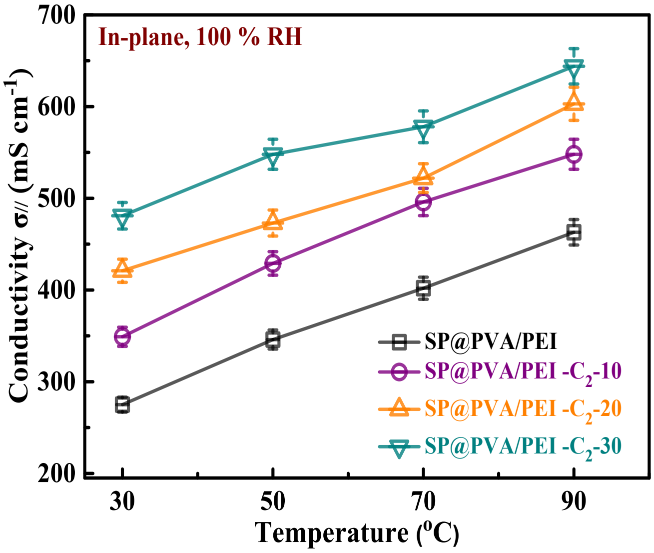

Fig. S17. Temperature-dependent in-plane conductivity ($\sigma_{//}$) of SP@PVA/PEI and SP@PVA/PEI/C_2-*Y* under 100% RH.

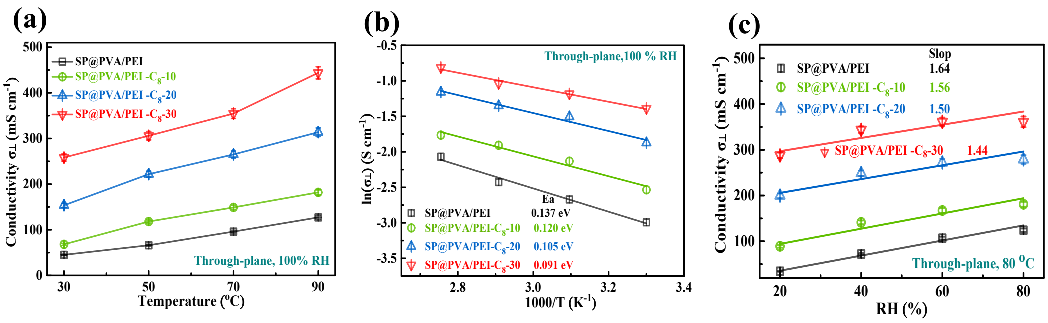

Fig. S18. (a) Temperature-dependent through-plane conductivity ($\sigma_{\perp}$) of SP@PVA/PEI and SP@PVA/PEI/C_8-Y under 100% RH. (b) Arrhenius-plots of through-plane conductivity ($\sigma_{\perp}$) under 100% RH. (c) RH-dependent through-plane conductivity ($\sigma_{\perp}$) of SP@PVA/PEI and SP@PVA/PEI/C_8-Y at 80 °C.

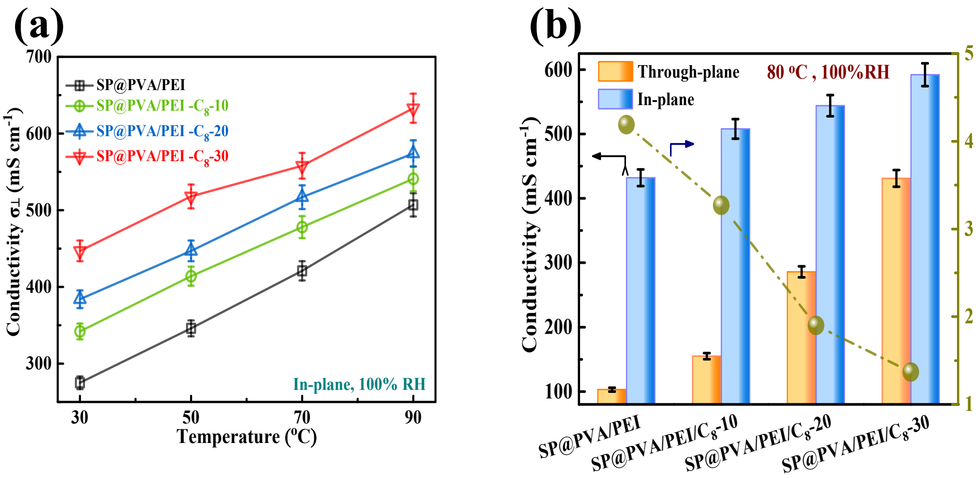

Fig. S19. (a) Temperature-dependent through-plane conductivity ($\sigma_{\perp}$) of SP@PVA/PEI and SP@PVA/PEI/C_8-*Y* under 100% RH. (b) Transfer anisotropy coefficient ($\sigma_{//}/\sigma_{\perp}$) at 80 °C and 100% RH.

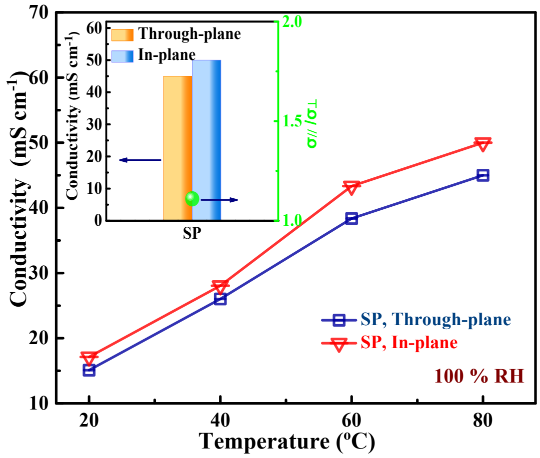

Fig. S20. Temperature-dependent through-plane conductivity ($\sigma_{\perp}$) and in-plane conductivity ($\sigma_{//}$) of SP under 100% RH (inset is the transfer anisotropy coefficient ($\sigma_{//}/\sigma_{\perp}$) of SP at 80 ^{o}C and 100 % RH).

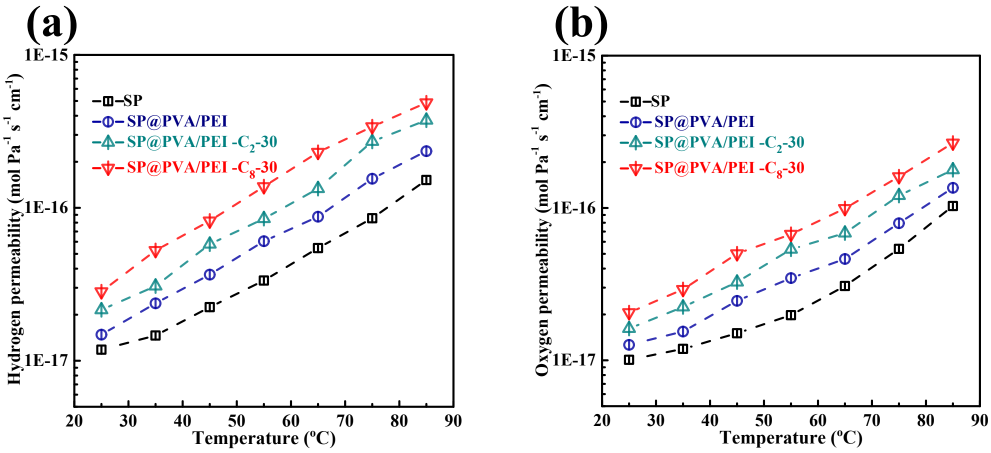

Fig. S21. (a) Hydrogen permeability and (b) oxygen permeability of SP, SP@PVA/PEI, SP@PVA/PEI/C_2-30, and SP@PVA/PEI/C_8-30 at different temperatures.

Table S1. Thickness of the membranes.

Membrane	SP@PVA/ PEI	SP@PVA/ PEI/C_2-10	SP@PVA/ PEI/C_2-20	SP@PVA/ PEI/C_2-30	SP@PVA/ PEI/C_8-10	SP@PVA/ PEI/C_8-20	SP@PVA/ PEI/C_8-30
Thickness (μm)	90±2	83±3	89±4	86±3	85±3	87±4	88±4

Table S2. Pore-structure parameters of nanofiber mats.

Sample	Surface area (m^2 g^{-1})	Total pore volume (cm^3 g^{-1})	Average pore diameter (nm)
PVA/PEI	7.35	0.031	-
PVA/PEI/C_2-10	22.47	0.093	17.13
PVA/PEI/C_2-20	45.76	0.209	20.94
PVA/PEI/C_2-30	78.83	0.287	34.75
PVA/PEI/C_8-10	17.16	0.152	19.27
PVA/PEI/C_8-20	39. 07	0.275	24.16
PVA/PEI/C_8-30	61.16	0.307	44.95

Table S3. Water state in nanofiber composite membranes.

Sample	Water uptake ω_t (wt. %)	Free water ω_f (wt. %)	Bound water ω_b (wt. %)	ω_b/ω_t
SP/PVA/PEI	25.7	17.0	8.7	33.8
SP/PVA/PEI/C_2-10	30.8	13.4	17.4	56.6
SP/PVA/PEI/C_2-20	33.9	5.8	28.1	82.9
SP/PVA/PEI/C_2-30	35.9	2.6	33.3	92.9

Table S4. Proton conduction behaviors of NFCMs in literatures.

Sample	In-plane $\sigma_{/\!/}$ (mS cm^{-1})	Through-plane $\sigma_{\perp}$ (mS cm^{-1})	$\sigma_{/\!/}/\sigma_{\perp}$	conditions	Ref.
Hybrid membranes					
Nafion / 3D sGO membranes	330	290	1.14	80 ^{o}C ,98%RH	[1]
Nafion / HNTs-SO_3H membranes	-	73	-	80 ^{o}C ,90%RH	[2]
Nafion / GO-Nafion membranes	-	82	-	95 ^{o}C ,100%RH	[3]
Pore materials membranes					
ABPBI / IL@SNR	-	65	-	80 ^{o}C ,98%RH	[4]
Asymmetric PBI / PPA	-	65.7	-	100 ^{o}C ,0%RH	[5]
CSPS / SPES	130	110	1.19		[6]
Nanofiber compote membranes					
SPPESK	80	7	11.1	30 ^{o}C, 100% RH	[7]
	165	37	4.55	80 ^{o}C, 100% RH	
SPEEK / Aquivion® membranes	~300	~200	1.50	80 ^{o}C, 100% RH	[8]
	~45	~30	1.50	80 ^{o}C, 40% RH	
6FDA-BDSA-r-APPF membrane	212	81	2.63	90 ^{o}C, 98% RH	[9]
Nafion / SPEEK/SiO_2 membrane	-	77	-	90 ^{o}C, 100% RH	[10]
CS / SPEEK membrane	-	60	-	120 ^{o}C, 0% RH	[11]
F-SPFEK membrane	-	61	-	80 ^{o}C, 100% RH	[12]
Nafion / PVDFNF membrane	-	91	-	90 ^{o}C, 95% RH	[13]
Nafion / PSSA-g-PVDFNF membrane	-	106	-	95 ^{o}C, 95% RH	[14]
Nafion / S-ZrO_2 fiber hybrid membrane	310	-	-	80 ^{o}C, 100% RH	[15]
single high-purity Nafion fiber membrane	1500	-	-	30 ^{o}C, 90% RH	[16]
SPES / Nafion membrane	-	88	-	25 ^{o}C, 95% RH	[17]
Nafion / SPEEK membrane	90	-	-	20 ^{o}C, 100% RH	[18]
CS / Nafion/PAN-C_2-25 membrane	270	150	1.81	120 ^{o}C, 0% RH	[19]
	-	~230	-	80 ^{o}C ,100% RH	
SP@PVA/PEI/C_8-30 membrane	592	397	1.49	80 ^{o}C,100% RH	This work
SP@PVA/PEI/C_2-30 membrane	609	561	1.08	80 ^{o}C,100% RH	This work

Supplementary References

1. L Cao, H. Wu, P. Yang, X. He, J. Li, Y. Li, M. Xu, M. Qiu and Z. Jiang, *Adv. Funct. Mater.*, 2018, **28**, 1804944.
2. I. Ressam, A. EI. Kadib, M. Lahcini, G. A. Luinstra and H. Perrot, *Int. J. Hydrogen Energy*, 2018, **43**, 18578–18591.
3. K. J. Peng, J. Y. Lai and Y. L. Liu, *J. Membr. Sci.*, 2016, **514**, 86–94.
4. X. Zhang, X. Fu, S. Yang, Y. Zhang, R. Zhang, S. Hu, X. Bao, F. Zhao, X. Li and Q. Liu, *J. Mater. Chem. A*, 2019, **7**, 15288–15301.
5. L.C. Jheng, S. L. C. Hsu, T. Y. Tsai and W. J. Y. Chang, *J. Mater. Chem. A*, 2014, **2**, 4225–4233.
6. C. Zhang, X. Yue, Y. Mu, X. Zuo, N. Lu, Y. Luo, R. Na, S. Zhang and G. Wang, *Electrochim. Acta*, 2019, **307**, 188–196.
7. M. Tanaka, Y. Takeda, T. Wakiya, Y. Wakamoto, K. Harigaya, T. Ito, T. Tarao and H. Kawakami, *J. Power Sources*, 2017, **342**, 125–134.
8. C. Boaretti, L. Pasquini, R. Sood, S. Giancola, A. Donnadio and M. Roso, *J. Membr. Sci.*, 2018, **545**, 66–74.
9. D. M. Yu, S. Yoon, T. H. Kim, J. Y. Lee, J. Lee and Y. T. Hong, *J. Membr. Sci.*, 2013, **446**, 212–219.
10. C. Lee, S. M. Jo, J. Choi, K. Y. Baek, Y. B. Truong, I. L. Kyratzis and Y.G. Shul, *J. Mater. Sci.*, 2013, **48**, 3665–3671.
11. J. Wang, Y. He, L. Zhao, Y. Li, S. Cao, B. Zhang and H. Zhang, *J. Membr. Sci.*, 2015, **482**, 1–12.
12. W. Liu, S. Wang, M. Xiao, D. Han and Y. Meng, *Chem. Commun.*, 2012, **48**, 3415–3417.
13. H. Y. Li and Y L. Liu, *J. Mater. Chem. A*, 2014, **2**, 3783–3793.
14. H. Y. Li, Y. Y. Lee, J. Y. Lai, and Y L. Liu, *J. Membr. Sci.*, 2014, **466**, 238–245.
15. Y. Yao, Z. Lin, Y. Li, M. Alcoutlabi, H. Hamouda and X. Zhang, *Adv. Energy Mater.*, 2011, **1**, 1133–1140.
16. B. Dong, L. Gwee, D. Salas-De La Cruz, K.I. Winey and Y. A. Elabd, *Nano Lett.*, 2010, **10**, 3785–3790.

17. I. Shabani, M. M. Hasani-Sadrabadi, V. Haddadi-Asl and M. Soleimani, *J. Membr. Sci.*, 2011, **368**, 233–240.
18. X. Xu, L. Li, H. Wang, X. Li and X. Zhuang, *RSC Adv.*, 2015, **5**, 4934–4940.
19. J. Wang, P. Li, Y. Zhang, Y. Liu, W. Wu and J. Liu, *J. Membr. Sci.*, 2019, **585**, 157–165.